Hysteresis and Bistability in a Realistic Cell Model for Calcium Oscillations and Action Potential Firing

J. M. A. M. Kusters,[1] J. M. Cortes,[1,2] W. P. M. van Meerwijk,[3] D. L. Ypey,[3] A. P. R. Theuvenet,[3] and C. C. A. M. Gielen[1]

[1]*Department of Biophysics, Radboud University Nijmegen, 6525 EZ Nijmegen, The Netherlands*

[2]*Institute for Adaptive and Neural Computation, School of Informatics, University of Edinburgh, EH1 2QL, United Kingdom*

[3]*Department of Cell Biology, Radboud University Nijmegen, 6525 ED Nijmegen, The Netherlands*

(Received 25 October 2006; published 1 March 2007)

Many cells reveal oscillatory behavior. Some cells reveal action-potential firing resulting from Hodgkin-Huxley (HH) type dynamics of ion channels in the cell membrane. Another type of oscillation relates to periodic inositol triphospate (IP3)–mediated calcium transients in the cytosol. In this study we present a bifurcation analysis of a cell with an excitable membrane and an IP3-mediated intracellular calcium oscillator. With IP3 concentration as a control parameter the model reveals a complex, rich spectrum of both stable and unstable solutions with hysteresis corresponding to experimental data. Our results reveal the emergence of complex behavior due to interactions between subcomponents with a relatively simple dynamical behavior.

DOI: 10.1103/PhysRevLett.98.098107 PACS numbers: 87.16.Ac, 05.45.−a, 05.70.Ln, 89.20.−a

Complexity and transitions among stable and unstable states are ubiquitous in biological systems [1,2]. In physics, instabilities in emerging collective properties have been studied for many years [3–6]. Recently, the phenomenon of multistability with hysteresis has also awakened a large interest in biology [7]. Instabilities, for instance, have been shown to be responsible for genetic alterations in tumor development [8] and for efficient information processing in the brain [9,10]. Multistable systems allow changes among different stable states. These transitions can be due to external input or due to instabilities which may serve as an alternative to switch between different branches of stable states [7]. Bistability is advantageous to prevent the system from reaching intermediate states. In addition, hysteresis may help to keep the system in a particular stable state, preventing it from sliding back to another state [11]. This is useful, for instance, in cell mitosis. Once initiated, it should not be terminated before completion [12].

At the network level, multistability plays an important role in cell signaling as well [13]. Communication between cells takes place at synaptic contacts, where an action-potential arrival releases a neurotransmitter, thus affecting the post-synaptic potential of the target cell. This information at the cell membrane is transferred to the cell nucleus by second messengers. Calcium is one such second messenger and calcium transients have been observed over a wide range of frequencies, with a chaotic or deterministic oscillating pattern [14].

Oscillatory behavior of cells is typically the result of two mechanisms. The first mechanism is located at the cell membrane and is related to periodic action-potential firing, usually triggered by input from other cells in the network. The other mechanism relates to oscillations in the concentration of free intracellular calcium by calcium release from the endoplasmic reticulum (ER) store. In this study we show how coupling of these two simple systems leads to a rich behavior with multiple stable and unstable states with hysteresis, in agreement with experimental observations. We present a simplified model, which captures the basic characteristics of normal rat kidney (NRK) fibroblasts reported in [15], and which reproduces the kinetics for both the membrane ionic currents and the intracellular calcium oscillator [16].

The dynamics of the NRK membrane potential depends on the sum of ion currents through the membrane:

$$\frac{dV_m}{dt} = -\frac{1}{C_m}\sum_i I_i, \tag{1}$$

where V_m is the membrane potential and $C_m = 20$ pF is the capacitance of the membrane. The most relevant currents are those through the inward rectifier potassium channel (I_{Kir}), the L-type Ca channels ($I_{\mathrm{Ca}L}$), Ca-dependent chloride channels ($I_{\mathrm{Cl(Ca)}}$), leak channels (I_{lk}), and SOC channels (I_{SOC}). The dynamics of the L-type Ca channel is given by $I_{\mathrm{Ca}L} = mhG_{\mathrm{Ca}L}\,(V_m - E_{\mathrm{Ca}L})$ with an activation (m) and inactivation (h) variable. The dynamics of m and h are described by first-order differential equations of the type

$$\frac{dx}{dt} = \frac{x_\infty(V_m) - x}{\tau_x(V_m)}, \tag{2}$$

where x_∞ and τ_x correspond to the steady-state (membrane potential dependent) (in)activation and time constant, respectively.

The Ca-dependent Cl current $I_{\mathrm{Cl(Ca)}}$ is given by

$$I_{\mathrm{Cl(Ca)}} = \frac{[\mathrm{Ca}^{2+}_{\mathrm{cyt}}]}{[\mathrm{Ca}^{2+}_{\mathrm{cyt}}] + K_{\mathrm{Cl(Ca)}}} G_{\mathrm{Cl(Ca)}}(V_m - E_{\mathrm{Cl(Ca)}}). \tag{3}$$

The Cl current increases with cytosolic calcium concentration $[\mathrm{Ca}^{2+}_{\mathrm{cyt}}]$, causing a depolarization to the Nernst

potential of Cl ions $E_{\mathrm{Cl(Ca)}}$ near -20 mV. For the definition of the other currents, see [17]; for details, see [15].

The flux of calcium through the membrane is the sum of the fluxes of Ca^{2+} ions through the L-type Ca channels and the SOC channel and by extrusion by the plasma membrane calcium ATPase (PMCA) pump $J_{\mathrm{PM}} = \frac{1}{z_{\mathrm{Ca}} F A_{\mathrm{PM}}} \times (I_{\mathrm{Ca}L} + I_{\mathrm{SOC}}) - J_{\mathrm{PMCA}}$.

Calcium in the cytosol is buffered by proteins in the cytosol. Buffering is described by first-order interactions between $[\mathrm{Ca}^{2+}_{\mathrm{cyt}}]$ and the concentration of the buffer

$$\frac{d[\mathrm{BCa}]}{dt} = k_{\mathrm{on}}([T_B] - [\mathrm{BCa}])[\mathrm{Ca}^{2+}_{\mathrm{cyt}}] - k_{\mathrm{off}}[\mathrm{BCa}], \quad (4)$$

where $[T_B]$ represents the total buffer concentration and [BCa] represents the concentration of buffered calcium.

The dynamics for the calcium concentration in the ER depends on the sum of fluxes through the IP3 receptor ($J_{\mathrm{IP3}R}$), leak through the ER membrane (J_{lkER}), and by (re)uptake by the sacroplasmic/endoplasmic reticulum calcium ATPase (SERCA) pump (J_{SERCA})

$$\frac{d[\mathrm{Ca}^{2+}_{\mathrm{ER}}]}{dt} = \frac{A_{\mathrm{ER}}}{\mathcal{V}_{\mathrm{ER}}}(-J_{\mathrm{IP3}R} - J_{\mathrm{lkER}} + J_{\mathrm{SERCA}}), \quad (5)$$

where the ratio of the surface A_{ER} and the volume $\mathcal{V}_{\mathrm{ER}}$ of the ER transforms the flux of Ca^{2+} ions through the ER membrane into changes of $\mathrm{Ca}^{2+}_{\mathrm{ER}}$ concentration. The flux through the IP3 receptor is described by

$$J_{\mathrm{IP3}R} = f_\infty^3 w^3 K_{\mathrm{IP3}R}([\mathrm{Ca}^{2+}_{\mathrm{ER}}] - [\mathrm{Ca}^{2+}_{\mathrm{cyt}}]), \quad (6)$$

where $[\mathrm{Ca}^{2+}_{\mathrm{ER}}] - [\mathrm{Ca}^{2+}_{\mathrm{cyt}}]$ is the concentration difference between calcium in the ER and in the cytosol. $K_{\mathrm{IP3}R}$ is the rate constant per unit area of IP3-receptor-mediated release. f_∞ and w represent the fraction of open activation and inactivation gates, respectively. The dynamics of f and w is given by Eq. (2), but since the time constant for f is fast, we use f_∞ instead of f. f_∞ and w_∞ depend both on the cytosolic calcium concentration:

$$f_\infty = \frac{[\mathrm{Ca}^{2+}_{\mathrm{cyt}}]}{K_{f\mathrm{IP3}} + [\mathrm{Ca}^{2+}_{\mathrm{cyt}}]}. \quad (7)$$

$$w_\infty = \frac{\frac{[\mathrm{IP_3}]}{K_{w\mathrm{IP_3}}+[\mathrm{IP_3}]}}{\frac{[\mathrm{IP_3}]}{K_{w\mathrm{IP_3}}+[\mathrm{IP_3}]} + K_{w(\mathrm{Ca})}[\mathrm{Ca}^{2+}_{\mathrm{cyt}}]}. \quad (8)$$

The excitable membrane and the IP3 oscillator are coupled by $[\mathrm{Ca}^{2+}_{\mathrm{cyt}}]$. During an action-potential opening of the L-type calcium channel causes a large inward current of Ca ions in the plasma membrane. The increased $[\mathrm{Ca}^{2+}_{\mathrm{cyt}}]$ activates the IP3 receptor by increasing f_∞ [Eq. (7)], causing an intracellular calcium transient. In the opposite process, IP3-mediated calcium oscillations cause periodic calcium transients, which open the Ca-dependent Cl channels [Eq. (3)]. The depolarization of the membrane towards the Nernst potential near -20 mV causes activation of the L-type Ca channels in the plasma membrane. After an action potential or Ca oscillation the reduction of cytosolic calcium by the activity of the SERCA and PMCA pump reduces $I_{\mathrm{Cl(Ca)}}$, such that the membrane repolarizes to the rest potential near -70 mV.

The dynamics of the complete single-cell model depends on the time evolution of the 7-dimensional vector $\vec{x}(t) = (m, h, w, [\mathrm{BCa}], V_m, [\mathrm{Ca}^{2+}_{\mathrm{cyt}}], [\mathrm{Ca}^{2+}_{\mathrm{ER}}])^T$. Using Eqs. (1), (2), (4), and (5) and keeping in mind the dependence of $[\mathrm{Ca}^{2+}_{\mathrm{cyt}}]$ on the Ca fluxes through cell membrane and ER membrane, this can be written as

$$\dot{\vec{x}}(t) = \vec{f}(\vec{x}(t)). \quad (9)$$

In order to find the stable states of $\vec{x}(t)$ it is important to notice that the cell behavior corresponds to an autonomous nonlinear dynamical system with periodic behavior. To find its stable periodic solutions we assume that $\tilde{\vec{x}}(t)$ is the periodic solution of the system in Eq. (9). For any perturbation $\vec{y}(t)$ around the stable periodic solution $\tilde{\vec{x}}(t)$ substitution of the solution $\vec{x}(t) = \tilde{\vec{x}}(t) + \vec{y}(t)$, Taylor expansion around the period solution $\tilde{\vec{x}}(t)$ and retaining only linear terms, gives

$$\dot{\vec{y}}(t) = J(\vec{x}(t))\vec{y}(t), \quad (10)$$

where $J(\vec{x}(t))$ is the Jacobian matrix $\nabla_{\vec{x}} f(\vec{x}(t))$ at the point $\vec{x}(t)$ on the periodic solution. The eigenvectors $\vec{y}_i(t)$ of J form the fundamental matrix $\Phi(t) = [\vec{y}_i(t), \vec{y}_2(t), \ldots, \vec{y}_n(t)]$. Any fundamental solution to the matrix of the T-periodic system in Eq. (10) can be written in the form $Y(t) = Z(t)e^{t\Phi}$, where Y, Z, and Φ are $n \times n$ matrices [18] with $Z(t) = Z(t+T)$. In particular, we can choose $Y(0) = Z(0) = I$, so that $Y(T) = Z(T)e^{T\Phi} = Z(0)e^{T\Phi}$. It then follows that the behavior of the solutions in the neighborhood of $\tilde{\vec{x}}(t)$ is determined by the eigenvalues of the matrix $e^{T\Phi}$. The (complex) eigenvalues λ_i of this matrix (the Floquet multipliers [18]) provide a measure of the local orbital divergence ($|\lambda_i| > 1$) or convergence ($|\lambda_i| < 1$) along a particular direction over one period of the periodic motion.

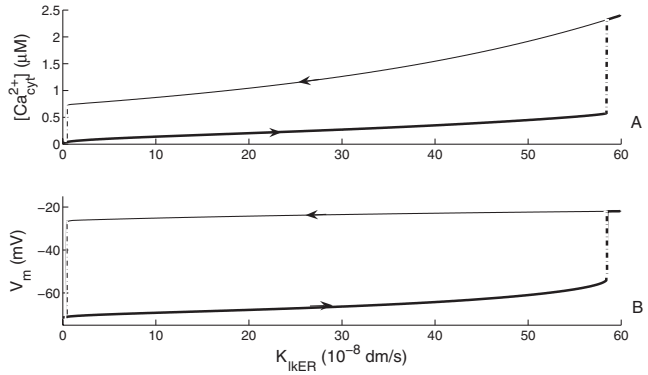

FIG. 1. Hysteresis diagram for the excitable membrane with K_{lkER} as a control parameter for the stable steady solutions for the calcium concentration in the cytosol (a) and membrane potential (b). Arrows show the direction of evolution of the system for increasing and decreasing values of K_{lkER}.

We will explore the bifurcation behavior and local stability of the electrically excitable membrane and intracellular calcium oscillator, separately, and then compare the results for a complete model, where the membrane oscillator and intracellular calcium oscillator are coupled, using the software packages AUTO [19] and XPP [19].

The excitable membrane can be studied in isolation by setting the IP3 concentration to zero to eliminate persistent intracellular calcium oscillations. The dynamics of the membrane is studied as a function of the leakage parameter K_{lkER} to produce variations in $[\mathrm{Ca}^{2+}_{\mathrm{cyt}}]$. Figure 1 shows the hysteresis diagram for the membrane with the steady states of $[\mathrm{Ca}^{2+}_{\mathrm{cyt}}]$ [Fig. 1(a)] and the membrane potential V_m [Fig. 1(b)]. $[\mathrm{Ca}^{2+}_{\mathrm{cyt}}]$ and V_m increase gradually until $K_{\mathrm{lkER}} \approx 58.0 \times 10^{-8}$ dm/s. Then the increased calcium concentration opens the Cl(Ca) channels and the membrane potential depolarizes to the Nernst potential of the Cl(Ca) channels close to -20 mV [see Fig. 1(b)]. This sudden depolarization opens the L-type Ca channels causing a calcium inflow through the membrane into the cytosol, which explains the sudden increase of $[\mathrm{Ca}^{2+}_{\mathrm{cyt}}]$ until 2.3 μM. When K_{lkER} is decreased, the L-type Ca channels are open, causing an increased $[\mathrm{Ca}^{2+}_{\mathrm{cyt}}]$. This explains why the Cl(Ca) channels are open and why the membrane potential remains near -20 mV. Only when $[\mathrm{Ca}^{2+}_{\mathrm{cyt}}]$ decreases to low concentrations, the Cl(Ca) channels close and the membrane potential repolarizes to -70 mV.

The dynamics of the intracellular calcium oscillator as a function of the IP3 concentration can be studied by blocking the L-type Ca channels ($G_{\mathrm{Ca}L} = 0$). The bifurcation diagram shows a stable state at low IP3 concentrations, followed by a subcritical Hopf bifurcation, where the IP3 receptor shows periodic oscillations (open/closed) and large calcium transients in the cytosol. The oscillation frequency increases with IP3 concentration until a subcritical Hopf bifurcation brings the system into a stable state where the IP3 receptor is continuously open with a constant leak of calcium into the cytosol; see [20,21].

The bifurcation diagram for the complete single-cell model is illustrated in Fig. 2, which shows cytosolic calcium concentration [Fig. 2(a)] and membrane potential [Fig. 2(b)] as a function of IP3. The solid and dashed lines represent stable and unstable states, respectively. For small IP3 values the cell has a single stable steady state. For IP3 > 0.15 μM the stable fixed point becomes unstable in a subcritical Hopf bifurcation. Calcium oscillations with action potentials [Fig. 2(b)] occur for IP3 $\in$ (0.15, 1.75) μM. In this regime, a rapid calcium inflow from the ER into the cytosol opens the Ca(Cl) channel, causing an inward current towards the Cl Nernst potential at -20 mV. After closure of the IP3 receptor, calcium is removed from the cytosol by Ca pumps in the cell membrane and ER, leading to repolarization to -70 mV. For IP3 > 1.75 μM, the fixed point $(\mathrm{Ca}_{\mathrm{cyt}}, V_m) \approx (3.00\ \mu\mathrm{M}, -20\ \mathrm{mV})$ becomes stable in a subcritical Hopf bifurcation. When IP3 is high, the IP3 receptor acts as a constant leak of calcium into the cytosol which opens the Ca(Cl) channels, causing a depolarization to the Cl Nernst potential near -20 mV [Fig. 2(b)].

If IP3 decreases, the cell reveals a complex hysteresis pattern. For decreasing IP3 concentrations, the system stays in a single stable steady state with $\mathrm{Ca}_{\mathrm{cyt}}$ near 3 μM and V_m near -20 mV until IP3 ≈ 0.85 μM. Then, crossing through a Hopf bifurcation causes instability (dashed

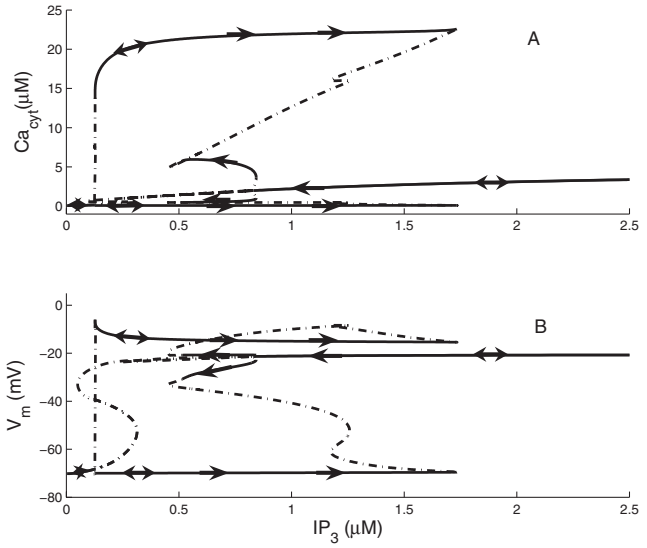

FIG. 2. Bifurcation diagram for the complete cell model with the cytosol calcium concentration (a) and membrane potential (b) as a function of IP3. Solid and dashed lines correspond to stable and unstable states, respectively. Arrows show the direction of evolution of the system for increasing and decreasing IP3 values.

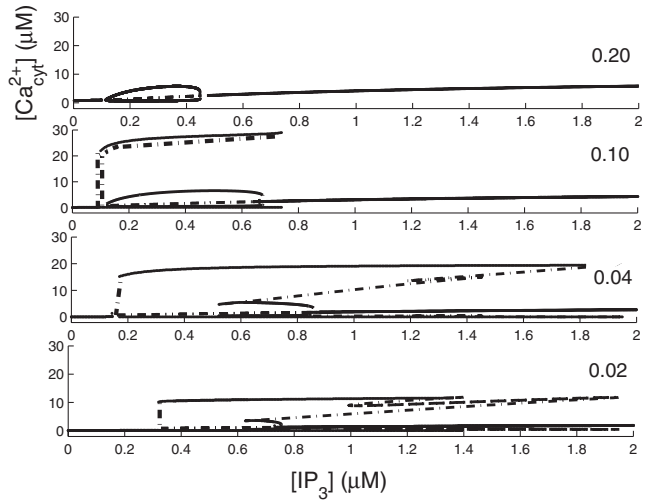

FIG. 3. Bifurcation diagrams for different values of G_{SOC}. Variations in $[\mathrm{Ca}^{2+}_{\mathrm{cyt}}]$ are due to both IP3-mediated calcium oscillations and action potentials for all G_{SOC} values except for $G_{\mathrm{SOC}} = 0.20$ nS, where the action potentials disappear. For values of G_{SOC} near 0.04 nS the IP3 range of hysteresis has a maximum.

line) forcing the system to behave as a stable oscillator with calcium oscillations (amplitude ≈ 6 μM) and small membrane potential oscillations around -20 mV. These oscillations are due to interaction between the L-type Ca channel and the IP3 receptor at elevated cytosolic calcium concentrations. At IP3 ≈ 0.45 μM the stable oscillator becomes unstable (dashed line), returning the system to the stable oscillations with large Ca transients and action potentials. Finally, for IP3 values below 0.15 μM the system returns to a single stable state.

Since the SOC channel in the plasma membrane plays a crucial role in stabilization of the calcium dynamics [15], we studied the dynamics of the cell as a function of the conductance of the SOC channel. Figure 3 shows the hysteresis diagrams for increasing values of G_{SOC}. As explained in [15], the cell behavior is unstable for $G_{\mathrm{SOC}} = 0.00$ nS with either depletion or accumulation of calcium in the ER. For small values of G_{SOC} bistability and hysteresis appear. The range of IP3 values with hysteresis is largest for G_{SOC} near 0.04 nS (see Fig. 3). For higher values of G_{SOC}, the range of hysteresis decreases until the typical Hopf bifurcation for the IP3-mediated calcium oscillations remains for $G_{\mathrm{SOC}} = 0.20$ nS.

The SOC conductance, which gives the largest hysteresis loop, corresponds to the observed SOC conductance in the literature [22,23] in the range from 0.04 to 0.05 nS. For hepatocytes SOC conductances are between (0.08,0.14) nS [24], but taking into account that the density of ionic channels in hepatocytes is twice as high as in fibroblasts [25], the range of SOC conductances which produce the largest amount of hysteresis is in agreement with values reported by [22,23].

The results in this Letter for NRK fibroblast cells are relevant for a wide class of cells. Interaction between an IP3-mediated intracellular calcium oscillator and action-potential generation to ensure stable propagation of waves of activity has also been demonstrated in many other cell types, such as interstitial cells of Cajal [26], β cells in the islets of Langerhans in the pancreas [27], and in sinoatrial nodal cells in the heart [28].

Summarizing, we have presented a model reproducing experimental data on calcium oscillations and action-potential generation. The emergence of complex behavior due to interactions between subcomponents with relatively simple dynamics illustrates the importance of studying a complete system, rather than the components in isolation, to understand the dynamics and functionality of a system.

We acknowledge financial support from the Netherlands Organization for Scientific Research, Engineering and Physical Sciences Research Council, and Ministerio de Educacion y Ciencia, Projects No. NWO 805.47.066, No. EPSRC EP/C0 10841/1, and No. MEC EX2005-0804.

[1] J. D. Murray, *Mathematical Biology I: An Introduction* (Springer, New York, 2002).
[2] *Foundations of Systems Biology*, edited by H. Kitano (MIT, Cambridge, MA, 2001).
[3] H. Haken, Rev. Mod. Phys. **47**, 67 (1975).
[4] B. J. T. Jones, Rev. Mod. Phys. **48**, 107 (1976).
[5] C. Normand, Y. Pomeau, and M. G. Velarde, Rev. Mod. Phys. **49**, 581 (1977).
[6] M. C. Cross and P. C. Hohenberg, Rev. Mod. Phys. **65**, 851 (1993).
[7] P. Ashwin and M. Timme, Nature (London) **436**, 36 (2005).
[8] C. Lengauer, K. W. Kinzler, and B. Vogelstein, Nature (London) **396**, 643 (1998).
[9] M. Rabinovich, A. Volkovskii, P. Lecanda, R. Huerta, H. D. Abarbanel, and G. Laurent, Phys. Rev. Lett. **87**, 068102 (2001).
[10] G. Laurent, M. S. R. W. Friedrich, M. I. Rabinovich, A. Volkovskii, and H. D. Abarbanel, Annu. Rev. Neurosci. **24**, 263 (2001).
[11] M. J. Solomon, Proc. Natl. Acad. Sci. U.S.A. **100**, 771 (2003).
[12] W. Sha, J. Moore, K. Chen, A. Lassaletta, C. S. Yi, J. J. Tyson, and J. C. Sible, Proc. Natl. Acad. Sci. U.S.A. **100**, 975 (2003).
[13] D. Angeli, J. E. Ferrell, and E. D. Sontag, Proc. Natl. Acad. Sci. U.S.A. **101**, 1822 (2004).
[14] T. R. Chay and J. Rinzel, Biophys. J. **47**, 357 (1985).
[15] J. M. A. M. Kusters, M. M. Dernison, W. P. M. van Meerwijk, D. L. Ypey, A. P. R. Theuvenet, and C. C. A. M. Gielen, Biophys. J. **89**, 3741 (2005).
[16] E. G. Harks, J. J. Torres, L. N. Cornelisse, D. L. Ypey, and A. P. Theuvenet, J. Cell Physiol. **196**, 493 (2003).
[17] The leak current is defined by $I_{\mathrm{lk}} = G_{\mathrm{lk}}(V_m - E_{\mathrm{lk}})$. The current through the SOC channel is given by $I_{\mathrm{SOC}} = \frac{K_{\mathrm{SOC}}}{[\mathrm{Ca}^{2+}_{\mathrm{cyt}}]+K_{\mathrm{SOC}}} G_{\mathrm{SOC}}(V_m - E_{\mathrm{SOC}})$. This current increases when the concentration of calcium in the ER decreases and plays an important role in calcium homeostasis of the cell.
[18] J. Guckenheimer and P. Holmes, *Nonlinear Oscillations, Dynamical Systems, and Bifurcations of Vector Fields* (Springer-Verlag, Berlin, 1983), Vol. 42.
[19] T. F. Fairgrieve and A. D. Jepson, SIAM J. Numer. Anal. **28**, 1446 (1991).
[20] S. Schuster, M. Marhl, and T. Hofer, European Journal of Biochemistry **269**, 1333 (2002).
[21] Y. Li and J. Rinzel, J. Theor. Biol. **166**, 461 (1994).
[22] A. B. Parekh and J. W. Putney, Physiol. Rev. **85**, 757 (2005).
[23] E. Krause, F. Pfeiffer, A. Schmid, and I. Schulz, J. Biol. Chem. **271**, 32 523 (1996).
[24] G. Y. Rychkov, T. Litjens, M. L. Roberts, and G. J. Barritt, Cell Calcium **37**, 183 (2005).
[25] Z. Yin and M. Watsky, Am. J. Physiol. Lung Cell Mol. Physiol. **288**, L1110 (2005).
[26] H. Cousins, F. Edwards, H. Hickey, C. Hill, and G. Hirst, J. Physiol. **550**, 829 (2003).
[27] O. Aslanidi, O. Mornev, A. Skyggebjerg, P. Arkhammar, O. Thastrup, M. Sorensen, P. Christiansen, K. Conradsen, and A. Scott, Biophys. J. **80**, 1195 (2001).
[28] V. A. Maltsev, T. M. Vinogradova, and E. G. Lakatta, J. Pharmacol. Sci. **100**, 338 (2006).